ELSEVIER

Biophysical Chemistry 134 (2008) 84–92

Biophysical Chemistry

http://www.elsevier.com/locate/biophyschem

Helix-rich transient and equilibrium intermediates of equine β-lactoglobulin in alkaline buffer

Yoshitaka Matsumura [a], Jinsong Li [a], Masamichi Ikeguchi [b], Hiroshi Kihara [a,*]

[a] *Department of Physics, Kansai Medical University, 18-89 Uyama-Higashi, Hirakata 573-1136, Japan*
[b] *Department of Bioinformatics, Faculty of Engineering, Soka University, Hachioji, Tokyo 192-8577, Japan*

Received 19 September 2007; received in revised form 19 January 2008; accepted 21 January 2008
Available online 13 February 2008

Abstract

Acidic buffer conditions are known to stabilize helix-rich states of even those proteins with a predominantly β-sheet native secondary structure. Here we investigated whether such states also exist under alkaline buffer conditions. The guanidine hydrochloride (GuHCl)-induced unfolding transition and kinetic refolding of equine β-lactoglobulin (ELG) by GuHCl-jump were investigated at pH 8.7 by far-ultraviolet circular dichroism. We found that an equilibrium intermediate appeared in 45% ethylene glycol (EGOH) buffer with 1.5 M GuHCl. The intermediate is rich in non-native α-helix, which is similar to the helix-rich state of ELG at pH 4.0. A kinetic study was done on the folding rate of ELG and compared with bovine β-lactoglobulin (BLG). Transient intermediates, which were observed as the burst phase of the refolding reaction, were also rich in α-helix. The activation enthalpy of ELG was calculated to be c.a. 80 kJ/mol, whereas that of BLG was c.a. 70 kJ/mol in the presence of 45% EGOH. The ellipticities of the transient intermediate of ELG show temperature dependence in the presence of 45% EGOH, whereas that of BLG did not show significant dependence.

This study therefore extends the existence of helix-rich equilibrium and transient intermediates of predominantly β-sheet proteins to alkaline buffer conditions.
© 2008 Elsevier B.V. All rights reserved.

Keywords: Protein folding; Equine β-lactoglobulin; Stopped-flow; Equilibrium intermediate; Transient intermediate

1. Introduction

β-lactoglobulin is one of the whey proteins found in milk [1]. Among β-lactoglobulins from various species, bovine β-lactoglobulin (BLG) has been most extensively studied [2]. Kuwajima found a non-native α-helix-rich kinetic intermediate on the BLG refolding pathway [3,4]. Arai et al. reported that the intermediate is a molten globule state, based on time-resolved x-ray scattering [5]. Qin et al. investigated the refolding of BLG at subzero temperatures, and found another intermediate prior to the appearance of the non-native α-helix-rich intermediate at −28 °C. The newly found intermediate is also rich in α-helix, but less so than the previously found intermediate [6].

Equine β-lactoglobulin (ELG) has several potential advantages over BLG for studying the pH dependent formation of thermodynamic or kinetic intermediates. Unlike BLG, it has no free cysteine residues that could interchange with disulfide bonds [7,8]. Also unlike BLG, it is monomeric from pH 1.5 to 8 [7,9]. The amino acid sequence homology of BLG and ELG is about 57% [10,11]. Both of the two β-lactoglobulins take the up-and-down β-barrel structure, which is consisted of eight β-strands and one α-helix [2,12,13].

Fujiwara et al. studied the kinetics and thermodynamics of ELG at pH 1.5 and 4.0, and reported a non-native α-helix-rich intermediate on the refolding pathway of ELG at pH 4.0 [14]. They also found an α-helix-rich equilibrium intermediate at the moderate denaturant concentrations at pH 4.0. These two

Abbreviations: ELG, equine β-lactoglobulin; CD, circular dichroism; far-UV, far-ultraviolet; EGOH, ethylene glycol; BLG, bovine β-lactoglobulin; GuHCl, guanidine hydrochloride.

* Corresponding author. Tel.: +81 72 856 2121; fax: +81 72 850 0733.
E-mail address: kihara@makino.kmu.ac.jp (H. Kihara).

0301-4622/$ - see front matter © 2008 Elsevier B.V. All rights reserved.
doi:10.1016/j.bpc.2008.01.010

intermediates are equivalent as far as circular dichroism (CD) measurements are concerned. Ikeguchi also performed thermodynamic study of ELG at pH 1.5, and found that the protein takes a molten globule state, which is equivalent to the kinetic and equilibrium intermediates observed at pH 4.0 [9,14].

Thermodynamic and kinetic intermediates richer in helix content than the native state have been reported for a number of proteins besides BLG and ELG [15–19]. In this study, we wanted to see if such helical structure can also be observed in alkaline solutions, not usually thought of as a condition enhancing helix stability. If so, this would demonstrate that transient formation of local secondary structure is a robust process during folding (kinetic experiments), and even low enough in free energy to manifest itself under equilibrium conditions (thermodynamic experiments).

Thus we conducted kinetic and thermodynamic studies of ELG at pH 8.7. In alkaline solution, we observed by stopped-flow a non-native α-helix-rich kinetic intermediate on the refolding pathway of ELG, as is the case at pH 1.5 and 4.0. The molecular ellipticity of the intermediate is −5400 deg cm^2 $dmol^{-1}$ at 222 nm, which is nearly equal to the values of the kinetic and the equilibrium intermediates at pH 4.0 [14]. We also detected an α-helix-rich thermodynamic intermediate at moderate guanidine hydrochloride (GuHCl) concentrations in the presence of 45% ethylene glycol (EGOH) at pH 8.7. The newly found equilibrium intermediate has a molecular ellipticity of c.a. −8000 deg cm^2 $dmol^{-1}$ at 222 nm, somewhat larger than the kinetic intermediate.

These results show that ELG is an excellent model system for investigating both transient and equilibrium intermediates of a monomeric β-sheet-rich protein over the full pH range. We conclude that even in alkaline solution, the propensity for ELG to form local secondary structure remains high.

Helix-rich intermediates have now been confirmed in 9 proteins under many different conditions, demonstrating that formation of misfolded local secondary structure is a common phenomenon during protein folding [18].

2. Materials and methods

2.1. Materials

ELG was purified from horse milk with slightly modified procedure from the previous work [9,20]. Recombinant ELG was expressed in *E. coli* and purified as described previously [13]. Purity of ELG was confirmed by SDS-PAGE, native-PAGE or tris-tricin PAGE [21].

Molecular weight of ELG is 18,500. The concentration of ELG was determined spectrophotometrically, using an extinction coefficient, ε = 12,000 M^{-1} cm^{-1} at 280 nm [9,22].

Crudely purified powder (mixture of BLG A and BLG B) was purchased from Sigma (Lot 124H7045). BLG A and BLG B were separated by anion-exchange chromatography through DEAE-Sephacel gel (Pharmacia) [23]. After the BLG A fraction and the BLG B fraction were dialyzed against distilled water, both of them were lyophilized. Each purified BLG A and BLG B was identified by native-PAGE. Both of them showed a single band. BLG A was used in the present experiments, and designated as BLG for simplicity hereafter.

Molecular weight of BLG is 18,400. The concentration of BLG was determined spectrophotometrically, using an extinction coefficient, $E^{1\%}_{.1\ cm}$ = 9.6 at 278 nm [24].

GuHCl is of ultra pure reagent grade from ICN Biomedicals Inc. (Lot 2345B). The concentration of GuHCl was calibrated by refractive index measurements [25,26]. The temperature was controlled within ±0.2 °C by a temperature controller ULT-80 of NESLAB.

2.2. Stopped-flow apparatus

The stopped-flow device was constructed for special use of high viscosity and low temperature in collaboration with Unisoku Inc [6,18,19]. Its dead time was estimated to be 5 ms by the reduction of 2, 6-dichloroindophenol by ascorbic acid at 4 °C and −28 °C (data not shown) [27].

2.3. CD measurements at equilibrium

The ELG samples were prepared in 50 mM phosphate buffer at pH 8.7 with various concentrations of GuHCl in the presence and absence of 45% EGOH, respectively. The concentration of ELG was 20–30 μM. CD measurements were performed at various temperatures with a spectropolarimeter specially designed by Unisoku Inc. Cuvettes of 1 mm path-length were used for all measurements.

2.4. Kinetic CD measurements

ELG was first unfolded in 50 mM phosphate buffer at pH 8.7 with 4.5 M GuHCl in the presence and absence of 45% EGOH, and then was diluted with seven times refolding buffer (0 M GuHCl) so as to initiate the refolding. The final concentration of GuHCl was 0.64 M, and the final concentration of ELG was 10–30 μM.

BLG was also first unfolded in 50 mM phosphate buffer, at pH 2 with 5 M GuHCl in the presence and absence of 45% EGOH and was diluted with seven times refolding buffer (0 M GuHCl) so as to initiate the refolding. The final concentration of GuHCl was 0.7 M, and the final concentration of BLG was 10–20 μM. The refolding process was monitored by CD at 222 ± 2 nm ($[\theta]_{222}$) at each temperature. Measurements were repeated and accumulated to get a good signal/noise ratio. The averaged data were normalized to give molar ellipticity. At each condition, in addition to the refolding experiments, two more experiments ('initial' and 'final') were always done; mixing the unfolded protein in the unfolded buffer with the same unfolded buffer. This gives us the 'initial' CD level. After the refolding experiments, we left the solution long time at the same condition, and then measured CD. This gives us the 'final' level. Usually, we measured the 'final' level 20 min after the folding reaction initiated.

Activation enthalpy of the folding reaction was obtained from the slope of logarithm of $k^*\eta$, where k is the rate constant of the observable phase and η is the viscosity of the solvent.

Activation enthalpy $\Delta H^{\ddagger}$ was calculated from the slope of logarithm of $k^*\eta$ *vs.* $1/T$ as follows according to Kramers equation [28,29].

$$k = \frac{C}{\eta}\exp\left(\frac{-\Delta G^{\ddagger}}{RT}\right)$$

where C is a constant, T is the absolute temperature, R is the gas constant and $\Delta G^{\ddagger}$ is activation free energy. From the equation, we can derive

$$\ln(k^*\eta) = -\frac{\Delta H^{\ddagger}}{RT} + \frac{\Delta S^{\ddagger}}{R} + \ln(C)$$

Then, when $\ln(k^*\eta)$ is plotted against $1/T$, we can obtain $\Delta H^{\ddagger}$ from the slope.

3. Results

3.1. Effect of EGOH on ELG conformation at equilibrium

We used EGOH as an anti-freeze at subzero temperatures. Then, we first investigated the effect of EGOH on the secondary structure of ELG at various temperatures by the measurement of far-ultraviolet (UV) CD. The far-UV CD spectra of ELG did not change in the presence of EGOH lower than 60%, whereas the spectra changed drastically in the presence of EGOH above 70%. In the inset figure of Fig. 1, are shown far-UV CD spectra of ELG at 0%, 30% and 90% EGOH concentrations at 4 °C, and the dependence of the ellipticity at 222 nm ($[\theta]_{222}$) on EGOH concentration at 4 °C is shown in Fig. 1. Results demonstrate that ELG takes an α-helix-rich conformation at EGOH concentrations above 70%. We have also observed CD spectra at −10 °C, −20 °C, and −28 °C, showing that ELG took native conformation at EGOH below 60% at subzero temperatures as at 4 °C (data not shown).

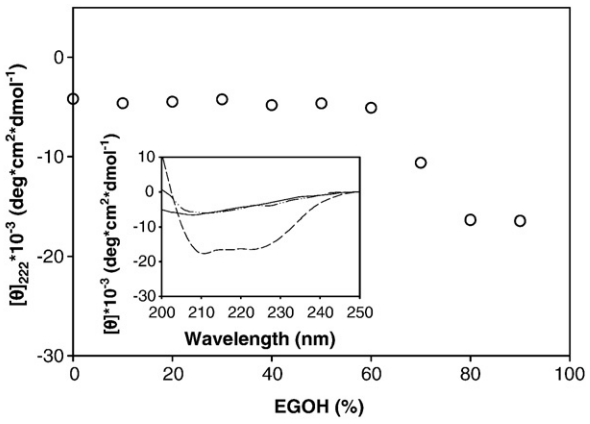

Fig. 1. $[\theta]_{222}$ dependence of EGOH concentration induced-ELG forming α-helices at pH 8.7 in 50 mM phosphate buffer at 4 °C. Inset: CD spectra of ELG at pH 8.7 in 50 mM phosphate buffer with different concentrations of EGOH at 4 °C. 0% EGOH (line), 30% EGOH (dash–dot–dot) and 90% EGOH (short dash).

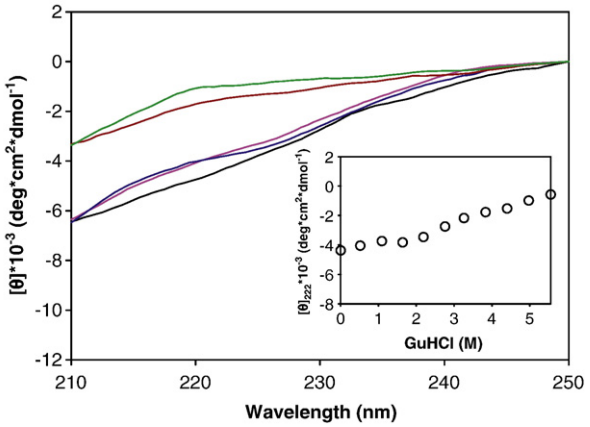

Fig. 2. CD spectra of ELG at pH 8.7 in 50 mM phosphate buffer with various concentrations of GuHCl at 4 °C. 0 M (black), 1.09 M (pink), 1.64 M (blue), 4.40 M (dark red) and 4.97 M (dark green). In short wavelength region, the data are not shown due to the absorption of GuHCl impurities. Inset: $[\theta]_{222}$ values of ELG unfolding are plotted against GuHCl concentrations at the same condition with the main figure.

3.2. ELG unfolding induced by GuHCl at equilibrium

Next, we performed ELG unfolding induced by GuHCl in 50 mM phosphate buffer at equilibrium. The far-UV CD spectra of ELG at pH 8.7 and at 4 °C were measured at various GuHCl concentrations. In Fig. 2, typical CD spectra at 4 °C are shown at GuHCl concentration of 0 M, 1.09 M, 1.64 M, 4.40 M and 4.97 M. The ellipticity at 222 nm ($[\theta]_{222}$) is plotted against GuHCl concentrations, and shown in the inset of Fig. 2. The curve shows a monotonic increase of ellipticity from 0 to 1 M of GuHCl, and shows a plateau from 1 M to 2 M. The ellipticity increased again above 2 M.

Fujiwara et al. reported the unfolding titration of ELG by urea at 25 °C and at pH 8.7 [30]. They reported a plateau at

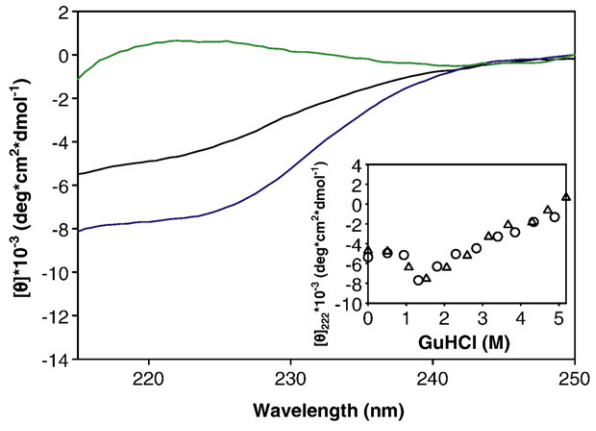

Fig. 3. CD spectra of ELG at pH 8.7 in 50 mM phosphate buffer and in the presence of 45% EGOH with various concentrations of GuHCl at −28 °C. 0 M (black), 1.53 M (blue) and 5.19 M (dark green). In short wavelength region, the data are not shown due to the absorption of GuHCl impurities. Inset: GuHCl concentration induced-ELG unfolding transitions monitored by $[\theta]_{222}$ at the same condition with the main figure (triangle). $[\theta]_{222}$ at 4 °C was also plotted in the inset (circle).

around 2–5 M of urea. Our result is at least qualitatively consistent with their report.

In contrast, CD spectra are significantly different in the presence of 45% EGOH. CD spectra were measured in the presence of 45% EGOH at various temperatures (4 °C, −10 °C, −20 °C and −28 °C). Typical CD spectra at −28 °C are shown at 0 M, 1.53 M and 5.19 M GuHCl in Fig. 3 and $[\theta]_{222}$ at 4 and −28 °C are shown in the inset of Fig. 3 as a function of GuHCl concentration. As seen in the inset figure, the ellipticity at 222 nm is nearly constant below 1 M, decreases with the increase of GuHCl concentration from 1 M to 1.5 M and then gradually increased above 2 M GuHCl at both temperatures, indicating an intermediate at 1.5 M GuHCl. It was also the case at −10 and −20 °C (data not shown). Fujiwara et al. measured

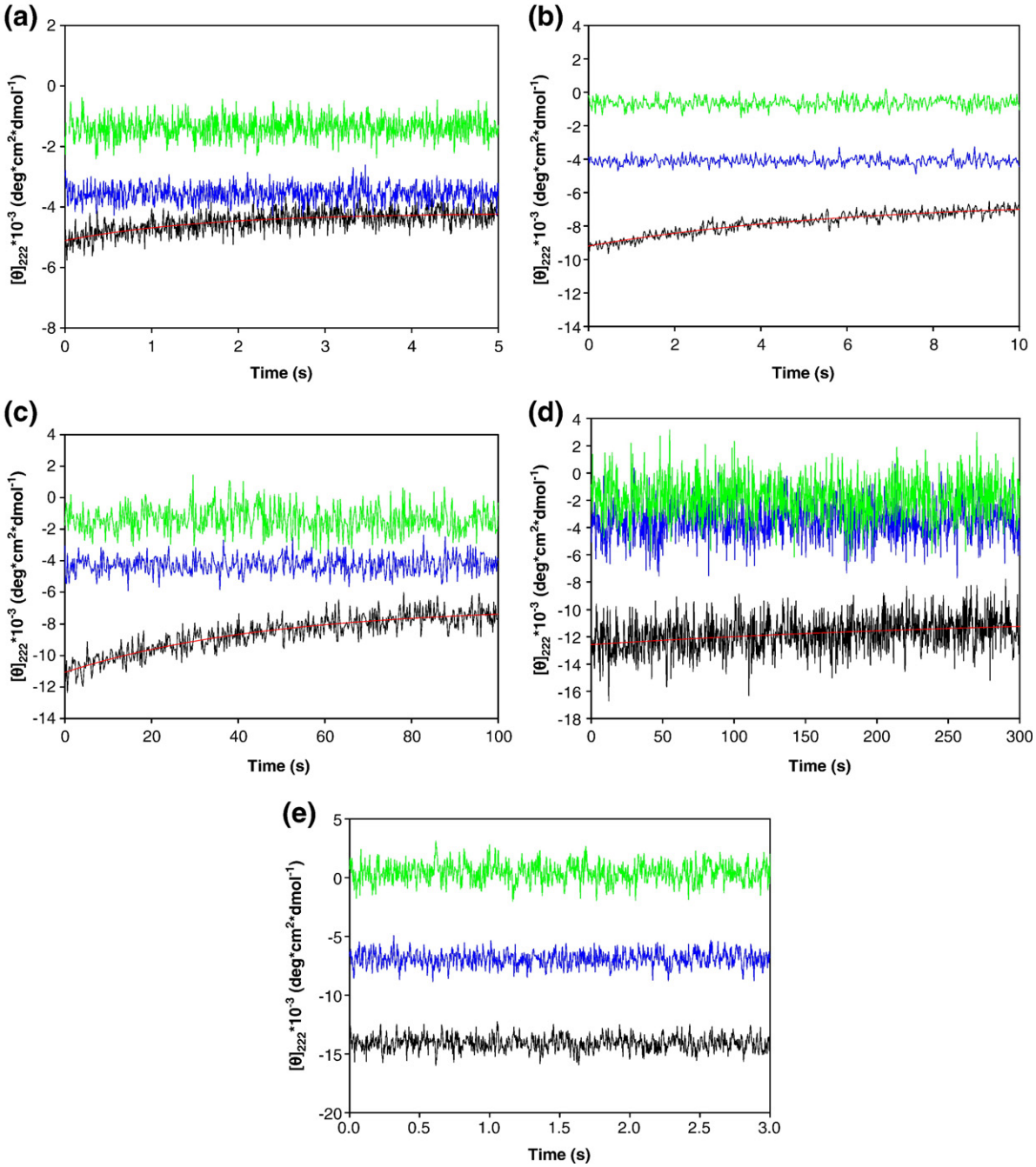

Fig. 4. Kinetic refolding curve (black) of ELG at pH 8.7 in 50 mM phosphate buffer. The refolding reaction was initiated by a concentration jump of GuHCl. The blue line represents the 'final' level, which was measured 20 min after the initiation of refolding. The green line shows the 'initial' level, where unfolded protein was mixed with the unfolded buffer. The red curve is the fitting curve. All of these results were repeated several times, and averaged curves are shown. Some of burst phases, the 'final' or 'initial' level ellipticities are a little different from Table 1 or Fig. 6. This is because two or three data of which time scale was different were not averaged in Fig. 4, but in Table 1 and Fig. 6, these different time-scaled data were also accumulated. (a) at 4 °C in the absence of 45% EGOH. The rate constant was $0.8 \pm 0.2\ s^{-1}$. (b) at 4 °C in the presence of 45% EGOH. The rate constant was $0.172 \pm 0.006\ s^{-1}$. (c) at −10 °C in the presence of 45% EGOH. The rate constant was $0.0237 \pm 0.003\ s^{-1}$. (d) at −20 °C in the presence of 45% EGOH. The rate constant was $0.00293 \pm 0.003\ s^{-1}$. (e) at −28.4 °C in the presence of 45% EGOH.

Table 1
Ellipticities of the burst phase, the 'initial' and the 'final' level, the 'final' level at infinity and the rate constants of ELG at pH 8.7

Buffer condition[a]	Temperature (°C)	Burst phase ellipticity (deg cm^2 dmol^{-1})	The final level (deg cm^2 dmol^{-1})	The initial level (deg cm^2 dmol^{-1})	The final level at ∞ (deg cm^2 dmol^{-1})[b]	Rate constant (s^{-1})
0% EGOH	4	−5400±300	−3300±400	−1100±400	−4300±100	0.8±0.2
45% EGOH	10	−6100±100	−3800±70	−1300±80	−4400±300	0.43±0.08
45% EGOH	4	−9200±400	−4100±1000	−700±100	−6400±1100	0.172±0.006
45% EGOH	−10	−13,200±1100	−4700±800	−100±600	−9800±1800	0.0237±0.003
45% EGOH	−15	−9800±200	−4200±70	−1200±80	−7300±400	0.0101±0.003
45% EGOH	−20	−12,800±200	−5200±1200	−100±900	−10,300±1600	0.00293±0.003

[a] Buffer: 50 mM phosphate buffer.
[b] These values were calculated according to the single exponential process at time infinity.

unfolding titration of ELG by urea and GuHCl at pH 4.0 and at 25 °C, and reported the presence of an intermediate [14]. Our finding of the intermediate on the unfolding titration induced by GuHCl in the presence of 45% EGOH is in agreement qualitatively with those obtained by Fujiwara et al. [14].

3.3. Kinetic refolding of ELG at pH 8.7

We carried out kinetic refolding experiments of ELG in the absence of EGOH at 4 °C and in the presence of 45% EGOH at various temperatures (10, 4, −10, −15, −20 and −28 °C). Refolding was initiated by mixing one volume of the unfolded ELG in the unfolded buffer (50 mM phosphate buffer with 4.5 M GuHCl) with 6 volumes of 50 mM phosphate buffer at 4 °C. Refolding experiments in the presence of EGOH were done, by mixing one volume of the unfolded ELG in 50 mM phosphate buffer with 45% EGOH and 4.5 M GuHCl with 6 volumes of 50 mM phosphate buffer with 45% EGOH. Results are shown in Fig. 4 (a)–(e). In all cases except at −28 °C, refolding traces showed the burst phase followed by an observable single exponential increase of ellipticity. Obtained ellipticities of the burst phase and the rate constants of the observable phase are summarized in Table 1. Both of the ellipticity of the burst phase and the rate constant of the observable phase decreased gradually with the decrease of temperature (Fig. 6 and Table 1). At 4 °C in the absence of EGOH, refolding trace reached to the 'final' value, indicating that no slower phases existed, whereas in other conditions, refolding trace did not reach to the 'final' value, indicating that the folding was not complete within the measuring time scale (Table 1 and Fig. 8).

At −28 °C, the refolding trace did not change within 3 s (Fig. 4 (e)). Qin et al. reported that the refolding of BLG at −28 °C showed two phases; the burst and a phase of decrease [6]. We repeated the refolding of BLG at the same condition with ELG, and found the same profiles for BLG, as shown in Fig. 5. The 'final' level of BLG was c.a. −6000 deg cm^2 dmol^{-1} at higher temperatures and decreased less than −10,000 deg cm^2 dmol^{-1} at lower temperatures (Fig. 9). This would indicate that the folding at lower temperatures were not finished yet even after 20 min.

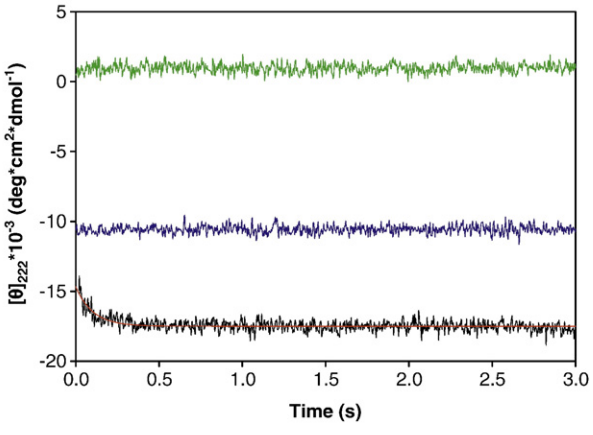

Fig. 5. Kinetic refolding curve (black) of BLG at pH 2 in 50 mM phosphate buffer and in the presence of 45% EGOH at −28.4 °C. The refolding reaction was initiated by a concentration jump of GuHCl. The blue line represents the 'final' level, which was measured 20 min after the initiation of refolding. The green line shows the 'initial' level, which was the mixing of the unfolded protein and the unfolded buffer. The red curve is the fitting curve. The rate constant was 7.8±2.9 s^{-1}.

4. Discussion

4.1. Effect of EGOH on ELG at equilibrium

ELG takes an α-helix-rich conformation with the mid point at 70% EGOH from the measurement of CD (Fig. 1). Above the 70% EGOH, the ellipticity at 222 nm was c.a. −17,000 deg cm^2 dmol^{-1}. BLG also takes an α-helix-rich conformation above 70% EGOH with the mid point at 75% EGOH. The ellipticity at 222 nm was reported as c.a. −25,000 deg cm^2 dmol^{-1} [6]. This indicates that the fraction of α-helix in ELG is significantly less than that of BLG.

The GuHCl-induced unfolding transition curve of BLG at pH 2.0 does not show significant changes in the presence and absence of 45% EGOH [6], whereas ELG takes an equilibrium intermediate at moderate GuHCl concentrations at pH 8.7 in the presence of 45% EGOH (Fig. 3), but not in the absence of EGOH. The ellipticity at 222 nm of the intermediate was c.a. −8000 deg cm^2 dmol^{-1}, which suggests the intermediate is rich in α-helix as is the case in the equilibrium intermediate observed by others at pH 4.0 and 1.5 [9,14].

We have estimated fractions of secondary structures of the equilibrium intermediate appearing at pH 8.7 in the presence of 45% EGOH with 1.5 M GuHCl by CONTIN program [31]. The results show fraction of α-helix=29%, fraction of

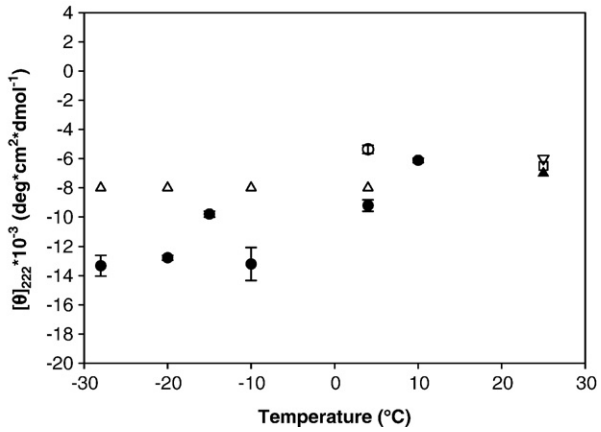

Fig. 6. Temperature dependence of the ellipticities of the burst phase of ELG monitored at 222 nm at pH 8.7. In 50 mM phosphate buffer without EGOH (○), in 50 mM phosphate buffer with 45% EGOH (●), the ellipticity at equilibrium at 1.5 M GuHCl in 50 mM phosphate buffer with 45% EGOH (△). The equilibrium intermediate at pH 1.5 (▲), at pH 4.0 (▽) and the kinetic burst at pH 4.0 (□) are plotted from Ref. [14] for comparison.

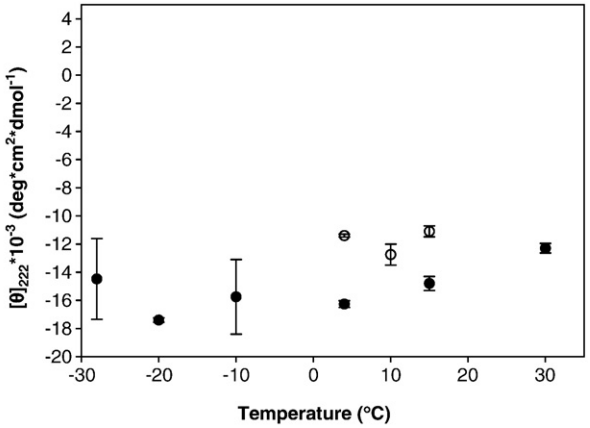

Fig. 7. Temperature dependence of the ellipticities of the burst phase of BLG monitored at 222 nm at pH 2. In 50 mM phosphate buffer without EGOH (○), in 50 mM phosphate buffer with 45% EGOH (●).

β-sheet=35% and fraction of random coil=37%. Secondary structure estimation was also done for the α-helix-rich conformation appearing at EGOH above 70%, of which fractions were 65%, 8% and 27%. From these values, we can conclude that the two conformations are different from each other.

4.2. The transient intermediate of ELG refolding

In all conditions, refolding kinetics show a burst phase within the dead time of the stopped-flow apparatus (Fig. 4), indicating the existence of a transient intermediate occurred within the dead time of the apparatus (5 ms). The ellipticities at 222 nm of the transient intermediates are summarized in Table 1 and shown in Fig. 6 as a function of measured temperatures. The ellipticity at 222 nm of the transient intermediate was −5400 deg cm^2 $dmol^{-1}$ at 4 °C in the absence of EGOH, indicating that the transient intermediate is rich in α-helix.

Fujiwara et al. reported that the transient intermediate appeared on the ELG folding pathway at pH 4.0 (25 °C) [14], of which ellipticity was around −6000 deg cm^2 $dmol^{-1}$. This value is also plotted in Fig. 6, as comparison. It is in good agreement with the present results.

The ellipticity at 222 nm of the transient intermediate was −6100 deg cm^2 $dmol^{-1}$ at 10 °C in the presence of 45% EGOH, and decreased with the decrease of temperature. At lower temperatures, the ellipticity reached to the constant value (−12,300 deg cm^2 $dmol^{-1}$) below −10 °C. The ellipticity change as a function of temperature might suggest the existence of the two different intermediates; one is more stable at higher temperatures and the other is more stable at lower temperatures. As comparison, the ellipticities at 222 nm of the similar transient intermediates of BLG were also measured, and their ellipticities are summarized in Table 2 and plotted in Fig. 7. They are nearly constant between 4 °C and −28 °C, while that at 30 °C is slightly larger. The ellipticities in the absence of EGOH seem to be slightly bigger than those in the presence of 45% EGOH.

4.3. The equilibrium intermediate and the transient intermediate

We have observed the equilibrium intermediate at 1.5 M GuHCl on the unfolding titration of GuHCl in the presence of 45% EGOH (Fig. 3). To compare this equilibrium intermediate and the transient intermediate described above, we also plotted ellipticities at 222 nm at equilibrium in the presence of 45% EGOH with 1.5 M GuHCl at various temperatures (Fig. 6). It should be noted that the ellipticities at 222 nm of the equilibrium intermediates are even lower than that at 1.5 M GuHCl

Table 2
Ellipticities of the burst phase, the 'initial' and the 'final' level and the rate constants of BLG at pH 2

Buffer condition [a]	Temperature (°C)	Burst phase ellipticity (deg cm^2 $dmol^{-1}$)	The final level (deg cm^2 $dmol^{-1}$)	The initial level (deg cm^2 $dmol^{-1}$)	Rate constant (s^{-1})
0% EGOH	15	−11,100±400	−5500±50	−1900±50	58.6±12.5
0% EGOH	10	−12,800±800	−5500±40	−1100±200	52.9±16.7
0% EGOH	4	−11,400±100	−6200±700	−1000±600	28.5±0.3
45% EGOH	30	−12,300±300	−5500±40	−2600±40	38.0±6.5
45% EGOH	15	−14,800±500	−5300±800	−2600±1100	11.0±4.3
45% EGOH	4	−16,300±200	−7000±500	−2000±100	6.1±1.1
45% EGOH	−10	−15,800±2700	−7800±300	−2500±2100	0.27±0.07
45% EGOH	−20	−17,400±200	−10,500±500	−2400±1400	0.062±0.001

[a] Buffer: 50 mM phosphate buffer.

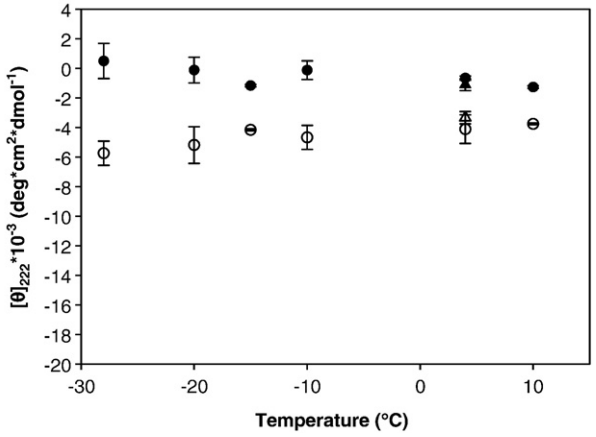

Fig. 8. Temperature dependence of the ellipticities of the 'final' and the 'initial' levels of ELG monitored at 222 nm at pH 8.7. The 'final' and 'initial' level ellipticities in 50 mM phosphate buffer without EGOH ('final';△, 'initial';▲), the 'final' and 'initial' level ellipticities in 50 mM phosphate buffer with 45% EGOH ('final';○, 'initial';●).

(we tried to obtain the ellipticity of the equilibrium intermediate based on the three-species-model fitting, but the results include large ambiguity). At 4 °C, the ellipticity at 222 nm at equilibrium in the presence of 45% EGOH with 1.5 M GuHCl and that of the transient intermediate in the presence of 45% EGOH fit well. The ellipticities at 222 nm at equilibrium in the presence of 45% EGOH with 1.5 M GuHCl did not change significantly with the decrease of temperature. Actually at −28 °C, the ellipticity at 222 nm at equilibrium in the presence of 45% EGOH with 1.5 M GuHCl was c.a. −8000 deg cm^2 dmol^{-1} and the ellipticity of the transient intermediate was c.a. −12,000 deg cm^2 dmol^{-1} (Fig. 6). It is then possible that the ellipticity of the equilibrium intermediate might be the same with one of the transient intermediates (the intermediate stable at higher temperature).

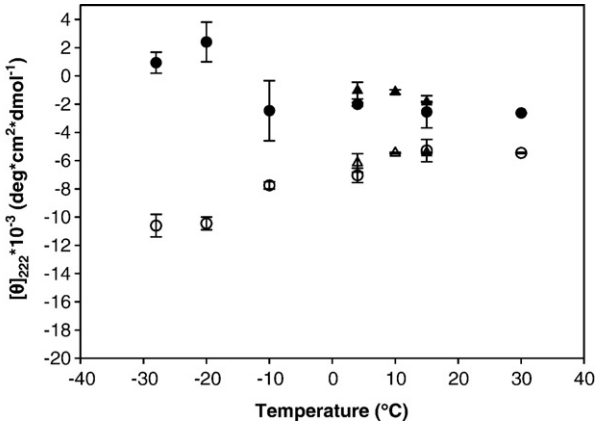

Fig. 9. Temperature dependence of the ellipticities of the 'final' and the 'initial' levels of BLG monitored at 222 nm at pH 2. The 'final' and 'initial' level ellipticities in 50 mM phosphate buffer without EGOH ('final';△, 'initial';▲), the 'final' and 'initial' level ellipticities in 50 mM phosphate buffer with 45% EGOH ('final';○, 'initial';●). At low temperatures, 'final' level ellipticities were less than −10,000 deg cm^2 dmol^{-1}. This indicates that BLG was not refolded to the native state 20 min after initiation of refolding, and this result is corresponding to Qin et al. reported [6].

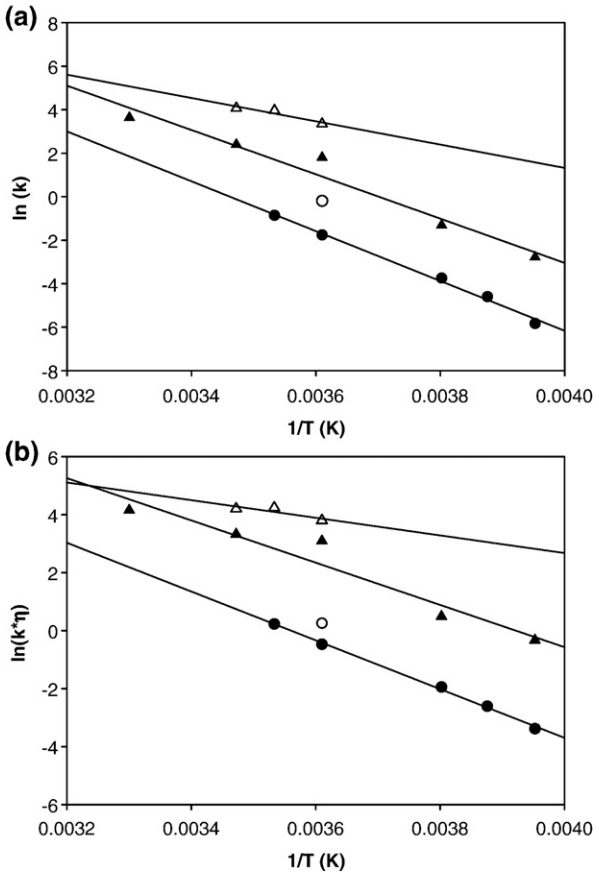

Fig. 10. Temperature dependence of the folding rate of ELG and BLG. (a) ln(k) *vs.* 1/T, and (b) ln($k^*\eta$) *vs.* 1/T, where k denotes the rate constant of the observable phases of ELG and BLG, and η is the viscosity of the solvent. ELG at pH 8.7 in 50 mM phosphate buffer without EGOH (○), ELG at pH 8.7 in 50 mM phosphate buffer with 45% EGOH (●), BLG at pH 2 in 50 mM phosphate buffer without EGOH (△), BLG at pH 2 in 50 mM phosphate buffer with 45% EGOH (▲). In case of BLG, refolding curve was fitted with a single or double exponential(s). When data were analyzed by double-exponential process, only the rate constants of the fast phases were plotted in the figure.

Fujiwara et al. speculated that the equilibrium intermediate has the same physicochemical properties as the one observed as the kinetically observed intermediate on the folding pathway at pH 4.0, 25 °C [14]. The equilibrium intermediate of ELG at moderate GuHCl concentrations observed at pH 8.7 in the presence of 45% EGOH has also similar properties to the transient intermediate as at pH 4.0.

In summary, ELG forms the equilibrium intermediate in the presence of 45% EGOH with 1.5 M GuHCl at pH 8.7 (present

Table 3
Activation enthalpy $\Delta H^{\ddagger}$ (kJ/mol) of ELG in the presence of 45% EGOH and BLG in the presence and absence of 45% EGOH

	ELG	BLG	
	45% EGOH	0% EGOH	45% EGOH
ln(k) *vs.* 1/T	95.5±4.2	44.7±15.2	85.0±9.8
ln($k^*\eta$) *vs.* 1/T	70.1±1.9	25.4±14.9	60.8±9.2
ln($k^*\eta^{0.7}$) *vs.* 1/T	77.8±2.6	31.1±15.0	68.0±9.3
ln($k^*(\sigma+\eta)$) *vs.* 1/T	81.0±2.3	39.9±14.9	72.6±8.9

study), and in the presence of moderate concentrations of urea and GuHCl at pH 4.0 [14]. Both take α-helix-rich conformation. ELG forms the transient intermediate in the presence and absence of 45% EGOH at pH 8.7 (present study) and in the absence of EGOH at pH 4.0 [14]. These two equilibrium intermediates and two transient intermediates take more or less similar α-helical content above 0 °C, whereas the transient intermediate at pH 8.7 takes higher α-helical content at the temperature lower than −10 °C. This demonstrates that the intermediates are more robust, and not the product only at acidic circumstances (Figs. 8 and 9).

4.4. A kinetic study of the transient intermediate

The folding rates of the observable phase in the presence of 45% EGOH decreased with the decrease of temperature (Table 1 and Fig. 10 (a)). Activation enthalpy $\Delta H^{\ddagger}$ of the ELG refolding was estimated from the slope, and is shown in Table 3. As the viscosity of the solution was temperature dependent, we also plotted logarithm of $k^*\eta$ of ELG, where k is the rate constant of the observable phase and η is the viscosity of the solvent against the reciprocal of temperature (Fig. 10 (b)). Both figures show good straight line against the reciprocal of temperature in the presence of 45% EGOH. Activation enthalpy $\Delta H^{\ddagger}$ was also estimated from the figures, and is shown in Table 3. There are several arguments to improve Kramers equation by using $\sigma+\eta$ or $\eta^{0.7}$ instead of η [29,32–39], where σ is the internal friction [39]. We have also plotted logarithm of $\log(k^*(\sigma+\eta))$ and $\log(k^*\eta^{0.7})$ against $1/T$ with $\sigma=4.1$ cP [39] , and obtained activation enthalpies of each case. They are also shown in Table 3.

In Fig. 10 (a) and (b), observable folding rates of BLG were also plotted both in the presence and absence of 45% EGOH. In the presence of 45% EGOH, logarithm of $k^*\eta$ shows a straight line against the reciprocal temperature, as is the case of ELG. Activation enthalpy $\Delta H^{\ddagger}$ of BLG were also calculated and are listed in Table 3.

$\Delta H^{\ddagger}$ of ELG in the presence of 45% EGOH was 95.5 kJ/mol from $\log(k)$ *vs.* $1/T$ plot, 70.1 kJ/mol from $\log(k^*\eta)$ *vs.* $1/T$ plot, 81.0 kJ/mol from $\log(k^*(\sigma+\eta))$ *vs.* $1/T$ plot, and 77.8 kJ/mol from $\log(k^*\eta^{0.7})$ *vs.* $1/T$ plot. Although our data are not sufficient to discuss which is the most appropriate value, the probable value is c.a. 80 kJ/mol. Activation enthalpies of BLG in the presence and absence of 45% EGOH were also estimated and are also listed in Table 3. The probable activation enthalpies are c.a. 70 kJ/mol and c.a. 35 kJ/mol, respectively. Thus, activation enthalpy of ELG is slightly higher than that of BLG in the presence of 45% EGOH.

4.5. Refolding of ELG and BLG at −28 °C

In BLG refolding process, a phase of α-helical increase was observed clearly at −28 °C as is Qin's data (Fig. 5 and [6]). Qin et al. [6] suggested that BLG formed a folding core at the early stage of BLG refolding from their experiments. Therefore, the present experiments also support his suggestion (Fig. 5). However, we could not monitor the same phase of α-helix increase on ELG folding pathway at −28 °C (Fig. 4 (e)). It would be explained because ELG folding core formation is finished within the dead time of the stopped-flow apparatus (5 ms).

Acknowledgement

The authors are grateful to Dr. Masayuki Morita of Kansai Medical University for kindly helping them prepare *E. coli* expression.

References

[1] R. Aschaffenburg, J. Drewry, Improved method for the preparation of crystalline b-lactoglobulin and a-lactalbumin from cow milk, Biochemistry 65 (1957) 273–277.
[2] G. Kontopidis, C. Holt, L. Sawyer, Invited review: β-lactoglobulin: binding properties, structure, and function, J. Dairy. Sci. 87 (2004) 785–796.
[3] K. Kuwajima, H. Yamaya, S. Miwa, S. Sugai, T. Nagamura, Rapid formation of secondary structure framework in protein folding studied by stopped-flow circular dichroism, FEBS Lett. 221 (1987) 115–118.
[4] K. Kuwajima, H. Yamaya, S. Sugai, The burst-phase intermediate in the refolding of β-lactoblobulin studied by stopped-flow circular dichroism and absorption spectroscopy, J. Mol. Biol. 264 (1996) 806–822.
[5] M. Arai, T. Ikura, G.V. Semisotnov, H. Kihara, Y. Amemiya, K. Kuwajima, Kinetic refolding of β-lactoblobulin. Studies by synchrotron x-ray scattering, and circular dichroism, absorption and fluorescence spectroscopy, J. Mol. Biol. 275 (1998) 149–162.
[6] Z.J. Qin, D.M. Hu, L. Shimada, T. Nakagawa, M. Arai, J.M. Zhou, H. Kihara, Refolding of β-lactoglobulin studied by stopped-flow circular dichroism at subzero temperatures, FEBS Lett. 507 (2001) 299–302.
[7] H.A. McKenzie, Milk proteins, Adv. Protein. Chem. 22 (1967) 55–234.
[8] P. Phelan, J. Paul, G. Malthouse, ^{13}C-n.m.r. of the cyanylated β-lactoglobulins: evidence that Cys-121 provides the thiol group of β-lactoglobulins A and B, Biochemistry 302 (1994) 511–516.
[9] M. Ikeguchi, S. Kato, A. Shimizu, S. Sugai, Molten globule state of equine β-lactoglobulin, Proteins 27 (1997) 567–575.
[10] A. Conti, J.G. Zimmermann, J. Liberatori, G. Braunitzer, D. Minori, The Primary structure of monomeric β-lactoglobulin I from horse colostrum (*Equus caballus*, perissodactyla), Hoppe-Seyler's Z, Physiol. Chem. 365 (1984) 1393–1401.
[11] T. Kobayashi, M. Ikeguchi, S. Sugai, Construction and characterization of β-lactoglobulin chimeras, Proteins 49 (2002) 297–301.
[12] H.L. Monaco, G. Zanotti, P. Spadon, M. Bolognesi, L. Sawyer, E.E. Eliopoulos, Crystal structure of the trigonal form of bovine beta-lactoglobulin and of its complex with retinol at 2.5 Å resolution, J. Mol. Biol. 197 (1987) 695–706.
[13] T. Kobayashi, M. Ikeguchi, S. Sugai, Molten globule structure of equine β-lactoglobulin probed by hydrogen exchange, J. Mol. Biol. 299 (2000) 757–770.
[14] K. Fujiwara, M. Arai, A. Shimizu, M. Ikeguchi, K. Kuwajima, S. Sugai, Folding–unfolding equilibrium and kinetics of equine β-lactoglobulin: equivalence between the equilibrium molten globule state and a burst-phase folding intermediate, Biochemistry 38 (1999) 4455–4463.
[15] Z. Qin, J. Ervin, E. Larios, M. Gruebele, H. Kihara, Formation of a compact structured ensemble without fluorescence signature early during ubiquitin folding, J. Phys. Chem. B 106 (2002) 13040–13046.
[16] E. Larios, J.S. Li, K. Schulten, H. Kihara, M. Gruebele, Multiple probes reveal a native-like intermediate during low-temperature refolding of ubiquitin, J. Mol. Biol. 340 (2004) 115–125.
[17] Z.J. Qin, S. Vyas, A.L. Fink, J.S. Li, H. Kihara, Transient a-helical structure during folding of src SH3 domain at subzero temperatures, J. Kansai Med. Univ. 58 (2006) 163–169.
[18] J. Li, M. Shinjo, Y. Matsumura, M. Morita, D. Baker, M. Ikeguchi, H. Kihara, An alpha-helical burst in the src SH3 folding pathway, Biochemistry 46 (2007) 5072–5082.

[19] J. Li, Y. Matsumura, M. Shinjo, M. Kojima, H. Kihara, A stable α -helix-rich intermediate is formed by a single mutation of the β-sheet protein, src SH3, at pH 3, J. Mol. Biol. 372 (2007) 747–755.
[20] S. Gohda, A. Shimizu, M. Ikeguchi, S. Sugai, The superreactive disulfide bonds in a-lactalbumin and lysozyme, J. Protein. Chem. 14 (1995) 731–737.
[21] W.F. Patton, N. Chung-Welch, M.F. Lopez, R.P. Cambria, B.L. Utterback, W.M. Skea, Tris-tricine and Tris-borate buffer systems provide better estimates of human mesothelial cell intermediate filament protein molecular weights than the standard Tris-glycine system, Anal Biochem. 197 (1991) 25–33.
[22] S.C. Gill, P.H. von Hippel, Calculation of protein extinction coefficients from amino acid sequence data, Anal. Biochem. 182 (1989) 319–326.
[23] F. Gervone, J.D. Brito, G.D. Prisco, F. Gerofano, L.G. Norona, S. Traniello, R. Zito, Simple procedures for the separation and identification of bovine milk whey proteins, Biochim. Biophys. Acta. 295 (1973) 555–563.
[24] S.N. Timasheff, R. Townend, Molecular interactions in β-lactoblobulin.VI. The dissociation of the genetic species of β-lactoblobulin at acid pH's, J. Am. Chem. Soc. 83 (1960) 470–473.
[25] C.N. Pace, Determination and analysis of urea and guanidine hydrochloride denaturation curves, Methods Enzymol. 131 (1986) 266–280.
[26] Y. Nozaki, The preparation of guanidine hydrochloride, Methods Enzymol. 26 (1972) 43–50.
[27] B. Tonomura, H. Nakatani, M. Ohnishi, M. Yamaguchi-Ito, K. Hiromi, Test reactions for a stopped-flow apparatus deduction of 2,6-dichlorophenolindophenol and potassium ferricyanide by L-ascorbic acid, Anal. Biochem. 84 (1978) 370–383.
[28] H.A. Kramers, Brownian motion in a field of force and the diffusion model of chemical reactions, Physica. 7 (1940) 284–304.
[29] M. Jacob, F.X. Schmid, Protein folding as a diffusional process, Biochemistry 38 (1999) 13773–13779.
[30] K. Fujiwara, M. Ikeguchi, S. Sugai, A partially unfolded state of equine β-lactoglobulin at pH 8.7, J. Protein. Chem. 20 (2001) 131–137.
[31] S.W. Provencher, J. Gloeckner, Estimation of globular protein secondary structure from circular dichroism, Biochmistry 20 (1981) 33–37.
[32] M. Jacob, T. Schindler, J. Balbach, F.X. Schmid, Diffusion control in an elementary protein folding reaction, Proc. Natl. Acad. Sci. U. S. A. 94 (1997) 5622–5627.
[33] D.K. Klimov, D. Thirumalai, Viscosity dependence of the folding rates of proteins, Phys. Rev. Lett. 79 (1997) 317–320.
[34] R.P. Bhattacharyya, T.R. Sosnick, Viscosity dependence of the folding kinetics of a dimeric and monomeric coiled coil, Biochemistry 38 (1999) 2601–2609.
[35] O. Bieri, J. Wirz, B. Hellrung, M. Schutkowski, M. Drewello, T. Kiefhaber, The speed limit for protein folding measured by triplet–triplet energy transfer, Proc. Natl. Acad. Sci. U. S. A. 96 (1999) 9597–9601.
[36] K.W. Plaxco, D. Baker, Limited internal friction in the rate-limiting step of a two-state protein folding reaction, Proc. Natl. Acad. Sci. U. S. A. 95 (1998) 13591–13596.
[37] S.A. Pabit, H. Roder, S.J. Hagen, Internal friction controls the speed of protein folding from a compact configuration, Biochemistry 43 (2004) 12532–12538.
[38] L. Qiu, S.J. Hagen, Internal friction in the ultrafast folding of the tryptophan cage, Chem. Phys. 312 (2005) 327–333.
[39] A. Ansari, C.M. Jones, E.R. Henry, J. Hofrichter, W.A. Eaton, The role of solvent viscosity in the dynamics of protein conformational changes, Science 256 (1992) 1796–1798.